Dynamics of slow fast predator–prey model of generalized Holling type III

Xiang Zhang (张 祥)

(Joint with **Cheng Wang**)

Shanghai Jiao Tong Uninversity

xzhang@sjtu.edu.cn

Advances in Qualitative Theory of Differential Equations

Castro Urdiales, SPAIN

June 21, 2019

Contents

Contents

slow system

$$\varepsilon \frac{dx}{d\tau} = \varepsilon \dot{x} = f(x, y, \varepsilon), \qquad \frac{dy}{d\tau} = \dot{y} = g(x, y, \varepsilon) \qquad (S)$$

$t = \tau/\varepsilon$ ⟺ $0 < \varepsilon \ll 1$

fast system

$$\frac{dx}{dt} = x' = f(x, y, \varepsilon), \qquad \frac{dy}{dt} = y' = \varepsilon g(x, y, \varepsilon) \qquad (F)$$

⇓ $\varepsilon \to 0$ (slow system)

$$0 = f(x, y, 0), \qquad \dot{y} = g(x, y, 0) \qquad (S1)$$

slow subsystem

⇓ $\varepsilon \to 0$ (fast system)

$$x' = f(x, y, 0), \qquad y' = 0 \qquad (F1)$$

fast subsystem

- The equilibria of fast subsystem $(F1)$ define the critical set

$$C := \{(x,y) \in \mathbb{R}^m \times \mathbb{R}^n |\ f(x,y,0) = 0\}.$$

  The curves given by C are called critical curves.
- If $C_0 \subset C$ is a manifold, we called C_0 a critical manifold.
- The regular orbits of the fast subsystem $(F1)$ are called fast orbits.

Normally hyperbolic

A compact submanifold $C_0 \subset C$ is called normally hyperbolic relative to fast subsystem $(F1)$ if all $p \in C_0$, the $m \times m$ matrix $(\mathrm{D}_x f)(p)$ has no eigenvalues with zero real part.

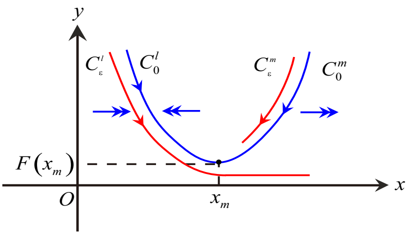

(a) A jump point $(x_m, F(x_m))$ (b) A canard point $(x_m, F(x_m))$

Figure 1.1: The local dynamics near the normally nonhyperbolic points.

- The U-shaped critical manifold C_0 (blue curve) consists of two sub-manifolds: C_0^l is attracting, while C_0^m is repelling.
- Double arrows (blue) indicate fast flow, and single arrows (blue) indicate slow flow.
- The slow manifolds C_ε^l and C_ε^m (red curve) of system (S) near the normally nonhyperbolic point $(x_m, F(x_m))$.

- A trajectory segment of system (S) is a canard if it follows an attracting slow manifold, passes close to a contact point of the critical manifold, and then follows a repelling slow manifold for $O(1)$ time on the slow time scale $\tau = t\varepsilon$.
- An orbit of system (S) lying in the intersection of the attracting slow manifold and the repelling slow manifold is called a maximal canard.

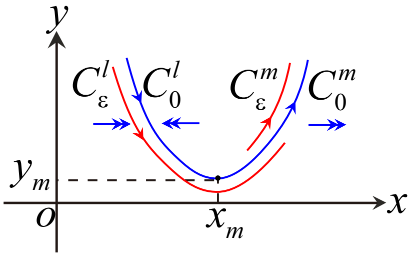

(a) A canard C_ε^l (b) A maximal canard C_ε

Given an ordered sequence of fast orbits and compact pieces of slow curves, oriented by the respective fast and slow subsystems, assuming their union is a topological circle, we call the sequence a slow-fast cycle (SFC).

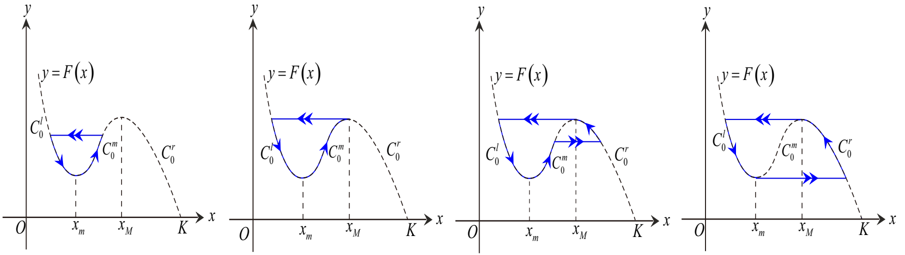

(c) A SFC without head (d) A transitory SFC (e) A SFC with head (f) A common SFC

Figure 1.2: Illustration of the family of slow-fast cycles (Solid blue).

- Denote by

  –$X_{\varepsilon,\lambda}$ the vector field associated to system (S).

  For a fixed $\lambda = \lambda_0$ and a SFC γ_0, if there are $\delta > 0$ and $\varepsilon_0 > 0$, such that for each $\varepsilon \in (0, \varepsilon_0)$ and $\lambda = \lambda(\varepsilon) \sim \lambda_0$, $X_{\varepsilon,\lambda}$ has a limit cycle $\gamma_\varepsilon^\lambda$ in the δ-neighborhood of γ_0, corresponding to $(\varepsilon, \lambda) = (0, \lambda_0)$, and $\gamma_\varepsilon^\lambda \to \gamma_0$ (in Hausdorff sense) as $\varepsilon \to 0$, then $\gamma_\varepsilon^\lambda$ is called a canard cycle, bifurcating from γ_0.

- The maximal number of such canard cycles, taking into account their multiplicities, is called the cyclicity of SFC γ_0 for $X_{\varepsilon,\lambda}$ at $(\varepsilon, \lambda) = (0, \lambda_0)$ and is denoted by $\mathrm{Cycl}(X_{\varepsilon,\lambda}, \gamma_0, (0, \lambda_0))$

- Relaxation oscillation is a periodic orbit of (S) which converges to a SFC consisting of alternating fast and slow segments forming a closed loop, where the slow ones have the same stability (e.g. Fig. 1.2 (d)) as $\varepsilon \to 0$.
- The very fast transition upon variation of a control parameter from a small amplitude limit cycle (Hopf cycle) via canard cycles to a large amplitude relaxation oscillation within an exponentially small range $O(\exp(-1/\varepsilon))$ of the control parameter is called canard explosion.

- GSPT was pioneered by Fenichel [JDE, 1979] and popularised by Jones [Lecture Notes in Math., 1995].
- The ideas in Fenichel [JDE, 1979] are based on the previous works Fenichel [Indiana Univ. Math. J., 71, 74, 77].

Fenichel's theorem

To state Fenichel's theorem, the following two assumptions are made:

- $(H1)$ Supose $f, g \in C^\infty$.
- $(H2)$ Suppose $C_0 \subseteq C$ is a compact normally hyperbolic manifold, possibly with boundary.

- For a normally hyperbolic critical manifold C_0, for each $p \in C_0$, assume that $\mathrm{D}_x f(p)$ has m_s eigenvalues with negative real part and m_u eigenvalues with positive real part where $m_s + m_u = m$.
- The local stable (unstable) manifold $W^s_{loc}(C_0)$ $(W^u_{loc}(C_0))$ can be written as

$$W^s_{loc}(C_0) := \bigcup_{p \in C_0} W^s_{loc}(p) \left(W^u_{loc}(C_0) := \bigcup_{p \in C_0} W^u_{loc}(p) \right).$$

  The manifolds $W^s_{loc}(p)$ $(W^u_{loc}(p))$ form a family of fast fibers for $W^s_{loc}(C_0)$ $(W^u_{loc}(C_0))$, with base points $p \in C_0$.
- Dim$(W^s_{loc}(C_0))$=$m_s + n$, Dim$(W^u_{loc}(C_0))$=$m_u + n$.

Fenichel's Theorem 1

For $0 < \varepsilon \ll 1$:

(i) For any $r < \infty$, there exists a C^r-smooth manifold C_ε, locally invariant under the flow of system (S), that is $\mathcal{O}(\varepsilon)$ close and C^r-diffeomorphic to C_0.

(ii) The flow on C_ε converges to the flow of system $(S1)$ on C_0 as $\varepsilon \to 0$.

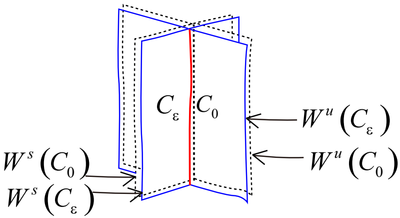

Figure 1.3: Fenichel's Theorem 1. Compact normally hyperbolic manifold C_0 (dashed black) perturbs C_ε (solid red).

Fenichel's Theorem 2

For $0 < \varepsilon \ll 1$, Fenichel's Theorem 1 holds and for any $r < \infty$, there exists a C^r-smooth stable and unstable manifold

$$W^s_{loc}(C_\varepsilon) = \cup_{p_\varepsilon \in C_\varepsilon} W^s_{loc}(p_\varepsilon), \quad W^u_{loc}(C_\varepsilon) = \cup_{p_\varepsilon \in C_\varepsilon} W^u_{loc}(p_\varepsilon),$$

locally invariant under the flow of system (S), that are $\mathcal{O}(\varepsilon)$ close and C^r-diffeomorphic to $W^s_{loc}(C_0)$ and $W^u_{loc}(C_0)$, respectively.

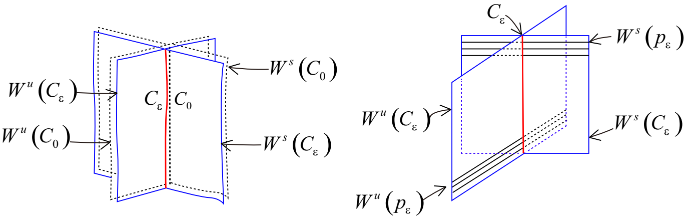

Figure 1.4: Fenichel's Theorem 2. $W^s_{loc}(C_0)$ and $W^s_{loc}(C_0)$ perturb to $W^s_{loc}(C_\varepsilon)$ and $W^s_{loc}(C_\varepsilon)$, respectively. $W^s_{loc}(C_\varepsilon)$ and $W^s_{loc}(C_\varepsilon)$ can be fibered.

Fenichel's Theorem 3

For $0 < \varepsilon \ll 1$, Fenichel's Theorem 2 holds and:

(i) For every $p_\varepsilon \in C_\varepsilon$, there is an m_s-dimensional manifold $W^s(p_\varepsilon) \subset W^s(C_\varepsilon)$, that is $\mathcal{O}(\varepsilon)$ close and C^r-diffeomorphic to $W^s(p)$.

(ii) The foliation $\{W^s_{loc}(p_\varepsilon) | p_\varepsilon \in C_\varepsilon\}$ is positively invariant, i.e. $W^s(p_\varepsilon) \cdot t \subset W^s(p_\varepsilon \cdot t)$ for all $t \geq 0$ such that $p_\varepsilon \cdot t \in C_\varepsilon$, where $\cdot t$ denotes the solution operator of system (S).

(iii) Similarly, (i) and (ii) hold for the unstable situation.

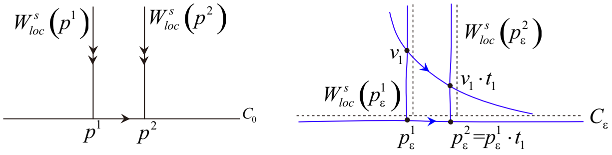

Figure 1.5: Fenichel's Theorem 3. The fibers $W^s(p_0)$ perturb to $W^s(p_\varepsilon)$ and $\{W^s_{loc}(p_\varepsilon) | p_\varepsilon \in C_\varepsilon\}$ is positively invariant.

Today, GSPT encompasses not only the results of Fenichel [JDE, 1979] but a much wider range of geometric technique, such as

- the blowup method,
- exchange lemma,
- slow-fast normal form theory,
- numerical methods,
- ....

- A breakthrough is Dumortier $\&$ Roussarie [Mem. AMS, 96], where the canard cycle in van del Pol's equation was studied by using blowup of singularities and foliation by center manifolds.
- Krupa (K.), Szmolyan (S.), Wechselberger (W.) and their coauthors developed the blowup method in studying the dynamics near the specific non-normally hyperbolic points of 2D and 3D slow-fast systems.

Dynamics near non-normally hyperbolic points of **2D** systems:

- K. & S., jump points and canard points, [SIMA, 2001],
- K. & S., relaxation oscillations and canard explosion, [JDE, 2001],
- K. & S., transcritical and pitchfork points, [Nonlinearity, 2001].

Dynamics near non-normally hyperbolic points of **3D** systems:

- S. & W., canards in $\mathbb{R}^3$, [JDE, 2001],
- S. & W., relaxation oscillations in $\mathbb{R}^3$, [JDE, 2004],
- W., a folded node, [SIADS, 2005],
- K. & W., a folded saddle-node type II, [JDE, 2010],
- Vo & W., a folded saddle-node type I, [SIMA, 2015],
- Mitry & W., folded saddles, [SIADS, 2017].

Based mainly on blowup method and slow divergence integral, De Maesschalck, Dumortier, Huzak, & Roussarie have a great deal of work on:

- stability loss delay, entry-exit function and dynamics near turning points,
- the mechanism of the birth of canard cycles and relaxation oscillations,
- cyclicity of slow-fast Hopf point and other singularities,
- cyclicity of different slow-fast cycles (canard, transitory, common),

See e. g., [Mem. AMS, 1996], [Trans. AMS, 2006], [Proc. Roy. Soc. Edinburgh, 2008], [Indag. Math., 2011], [JDE, 2001-2016], [DCDS, 2007a, 2007b, 2009].

Many blowup method calculations follow the five steps outlined next:

1. Find a suitable blowup map to desingularize the fold point (obtain additional hyperbolicity).
2. Find charts to express the blowup in local coordinates.
3. Investigate the dynamics of the blown-up vector fields in each chart.
4. Connect the results from different charts.
5. Blow down.

Example: Investigate the dynamics near the non-normally hyperbolic point $(0,0)$ of $x' = x^2 - y,\ y' = -\varepsilon$ using blowup map $(x, y, \varepsilon) = (\bar{r}\bar{x}, \bar{r}^2\bar{y}, \bar{r}^3\bar{\varepsilon})$.

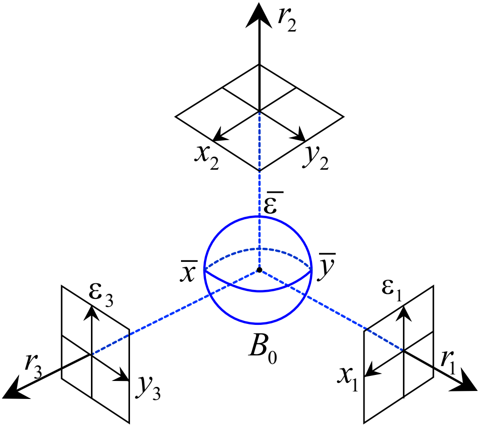

Figure 1.6: Geometrical interpretation of the blowup method.

Exchange Lemma can be used to understand how trajectories enter and leave the vicinity of a critical manifold.

- Exchange Lemma was first recognized by Jones & Kopell [JDE, 1994]. An excellent introduction to Exchange Lemma is Jones [Lecture Notes in Math., 1995].
- The exponentially-small-error version can be found in Jones, Kaper & Kopell [SIMA, 1996], see also the review Jones & Kaper [IMA Vol. Math. Anal., 2001].

The above Exchange Lemma requires the normally hyperbolicity of the critical manifold.

- W. S. Liu extended Exchange Lemma for loss-of-stability turning points [JDE, 2000; SIAP, 2005; DCDS, 2005; JDDE, 2006].
- Schecter proved Generalized Exchange Lemma for normally hyperbolic invariant manifold with rectifiable slow flow, loss-of-stability turning points and gain-of-stability turning points [JDE, 2008a, 2008b].
- Further studies on Generalized Exchange Lemma, see Jones & Tin [DCDS, 2009].

Predator-Prey models of Holling type III

- H. I. Freedman and R. M. Mathsen in [BMB,1993] proposed the following ratio-dependent predator-prey model

$$\begin{aligned} \dot{x} &= rx\left(1-\frac{x}{K}\right)-yp(x), \\ \dot{y} &= sy\left(1-\frac{y}{hx}\right), \end{aligned} \tag{2.1}$$

  with generalized Holling type III functional response $p(x)=\frac{mx^2}{ax^2+bx+1}$, where $x>0$ and $y\geq 0$ denote prey and predator densities, respectively.

- $r,s>0$: intrinsic prey and predator growth rate, respectively.
  $K>0$: prey environmental carrying capacity.
  $h>0$: $\frac{1}{h}$ is the number of prey required to support one predator.

- H. I. Freedman and R. M. Mathsen in [BMB,1993] proposed the following ratio-dependent predator-prey model

$$\begin{aligned} \dot{x} &= rx\left(1-\frac{x}{K}\right)-yp(x), \\ \dot{y} &= sy\left(1-\frac{y}{hx}\right), \end{aligned} \tag{2.1}$$

  with generalized Holling type III functional response $p(x)=\frac{mx^2}{ax^2+bx+1}$, where $x>0$ and $y\geq 0$ denote prey and predator densities, respectively.

- $r, s > 0$: intrinsic prey and predator growth rate, respectively.
  $K > 0$: prey environmental carrying capacity.
  $h > 0$: $\frac{1}{h}$ is the number of prey required to support one predator.

- For predator and prey, a functional response is the intake rate of a predator as a function of prey density.

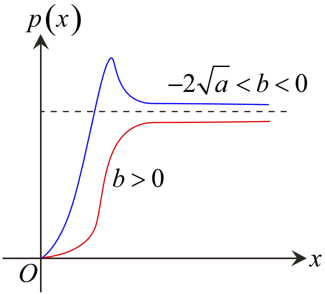

Figure 2.1: Geometrical interpretation of the generalized Holling type III functional response $p(x) = \frac{mx^2}{ax^2+bx+1}$, $(b > -2\sqrt{a}, a > 0, m > 0)$

- $b > -2\sqrt{a}$: so that $ax^2 + bx + 1 > 0$ for all $x \geq 0$ and hence $p(x) > 0$ for all $x > 0$.

- For predator and prey, a functional response is the intake rate of a predator as a function of prey density.

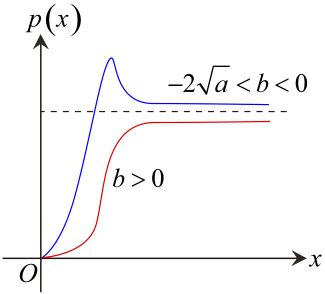

Figure 2.1: Geometrical interpretation of the generalized Holling type III functional response $p(x) = \frac{mx^2}{ax^2+bx+1}$, $(\underline{b > -2\sqrt{a}}, a > 0, m > 0)$

- $b > -2\sqrt{a}$: so that $ax^2 + bx + 1 > 0$ for all $x \geq 0$ and hence $p(x) > 0$ for all $x > 0$.

- By applying Dulac's criterion and constructing Lyapunov functions, Hsu $\&$ Huang investigated the global stability of an equilibrium of system (2.1) in [SIAM J. Appl. Math., 55(3):763-783, 1995].
- Based on the normal form theory and the center manifold theory, Huang, Ruan $\&$ Song considered the subcritical Hopf and B-T bifurcations of system (2.1) in [J. Differential Equations, 257(6):1721-1752, 2014].

- By applying Dulac's criterion and constructing Lyapunov functions, Hsu $\&$ Huang investigated the global stability of an equilibrium of system (2.1) in [SIAM J. Appl. Math., 55(3):763-783, 1995].
- Based on the normal form theory and the center manifold theory, Huang, Ruan $\&$ Song considered the subcritical Hopf and B-T bifurcations of system (2.1) in [J. Differential Equations, 257(6):1721-1752, 2014].

- By applying Dulac's criterion and constructing Lyapunov functions, Hsu & Huang investigated the global stability of an equilibrium of system (2.1) in [SIAM J. Appl. Math., 55(3):763-783, 1995].
- Based on the normal form theory and the center manifold theory, Huang, Ruan & Song considered the subcritical Hopf and B-T bifurcations of system (2.1) in [J. Differential Equations, 257(6):1721-1752, 2014].

Our results

By geometric singular perturbation theory (GSPT), we obtain:

- global asymptotical stability,
- singular Hopf bifurcation and canard explosion,
- canard cycles,
- relaxation oscillations,
- heteroclinic and homoclinic orbits,
- cyclicity of slow-fast cycles.

Dimensionless form

System (2.1) is topologically equivalent to the system

$$\begin{aligned} \frac{\mathrm{d}\bar{x}}{\mathrm{d}t} &= \bar{x}^2\left(\bar{x}^2+\bar{b}\bar{x}+1\right)\left(1-\frac{\bar{x}}{\bar{K}}\right)-\bar{x}^3\bar{y}, \\ \frac{\mathrm{d}\bar{y}}{\mathrm{d}t} &= \varepsilon\bar{y}(\bar{x}^2+\bar{b}\bar{x}+1)\left(\bar{x}-\bar{h}\bar{y}\right), \end{aligned} \tag{2.2}$$

with $(\varepsilon, \bar{K}, \bar{h}) \in \mathbb{R}^3_+$ and $\bar{b} > -2$, where

$$\bar{b} = \frac{b}{\sqrt{a}}, \quad \bar{K} = K\sqrt{a}, \quad \bar{h} = \frac{ra}{mh} \quad \text{and} \quad \varepsilon = \frac{s}{r}.$$

In the following, we drop the bars for notational convenience in system (2.2).

- An important feather of biological systems is that they often evolve on multiple scales.
- For example, hares and squirrels reproduce much faster than their predators, such as lynx and coyotes.
- Multiple scales problems of biological systems are usually modeled by slow-fast systems.

- An important feather of biological systems is that they often evolve on multiple scales.
- For example, hares and squirrels reproduce much faster than their predators, such as lynx and coyotes.
- Multiple scales problems of biological systems are usually modeled by slow-fast systems.

- An important feather of biological systems is that they often evolve on multiple scales.
- For example, hares and squirrels reproduce much faster than their predators, such as lynx and coyotes.
- Multiple scales problems of biological systems are usually modeled by slow-fast systems.

- The parameter ε in system (2.2) can be interpreted as the ratio between the intrinsic growth rate of the predator and the intrinsic growth rate of the prey.
- If the predator lives a very long time and encounters many different generations of prey, it is a natural assumption that $\frac{s}{r}$ is sufficiently small, i.e., $0 < \varepsilon \ll 1$.

- The parameter ε in system (2.2) can be interpreted as the ratio between the intrinsic growth rate of the predator and the intrinsic growth rate of the prey.
- If the predator lives a very long time and encounters many different generations of prey, it is a natural assumption that $\frac{s}{r}$ is sufficiently small, i.e., $0 < \varepsilon \ll 1$.

Critical manifold

$$C_0 := \left\{ (x,y) | y = F(x) := \frac{1}{x}\left(x^2 + bx + 1\right)\left(1 - \frac{x}{K}\right) \right\}.$$

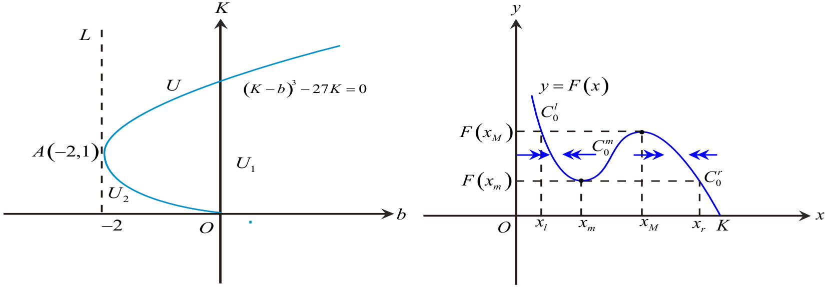

(a) $U := \{(b,K) \mid (K-b)^3 - 27K > 0\}$ (b) Dynamics of fast subsystem

Figure 2.2: The critical manifold C_0 (blue curve) is S-shaped when $(b,K) \in U$.

Let $A = (\frac{K}{h}+b-K)^2+3(Kb-1)$, $B = 2(\frac{K}{h}+b-K)^3-9(1-Kb)(\frac{K}{h}+b-K)-27K$ and $\Delta := B^2-4A^3$.

Existence of positive equilibria

(a) If $\Delta > 0$, then system (2.2) has a unique elementary anti-saddle.

(b) If $\Delta = 0$ and

- (b_1) $A > 0$ and $(\frac{K}{h}+b-K)+\sqrt{A} > 0$, then system (2.2) has a unique elementary anti-saddle;
- (b_2) $A = 0$, then system (2.2) has a unique degenerate equilibrium $(-\frac{1}{3}(\frac{K}{h}+b-K), -\frac{1}{3h}(\frac{K}{h}+b-K))$.

Existence of positive equilibria

(c) If $\Delta = 0$, $A > 0$ and $(\frac{K}{h} + b - K) + \sqrt{A} < 0$, then system (2.2) has two different positive equilibria.

(d) If $\Delta < 0$, $\frac{K}{h} < K - b - \sqrt{3(1 - Kb)}$ and $-2 < b < \frac{1}{K}$, then system (2.2) has three different positive equilibria.

In the following, for notational convenience, we let

$$S_1 := \{(K, b, h) | (K, b) \in U \text{ and } (a) \text{ or } (b) \text{ holds}\},$$

$$S_2 := \{(K, b, h) | (K, b) \in U \text{ and } (c) \text{ holds}\},$$

$$S_3 := \{(K, b, h) | (K, b) \in U \text{ and } (d) \text{ holds}\}.$$

Positive invariance

- The set $\Xi = \{(x, y) \in \mathbb{R} \times \mathbb{R} : 0 < x \leq K; 0 \leq y \leq K/h\}$ is positively invariant for system (2.2).
- Moreover, if $(b, K) \in U$, the set Ξ is global attracting in the first quadrant of the (x, y) plane for $0 < \varepsilon \ll 1$.

Dynamics near the origin

The origin $O(0,0)$ of system (2.2) is a non-hyperbolic saddle for all values of the parameters and $0 < \varepsilon \ll 1$.

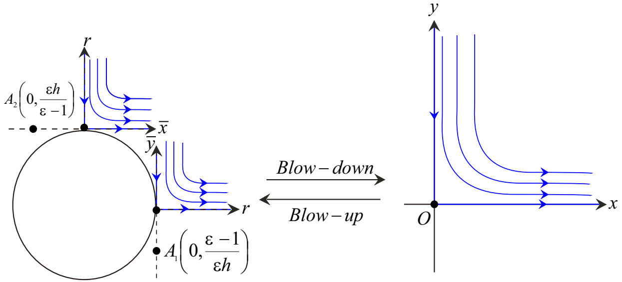

Figure 2.3: Directional blow-up at the origin $O(0,0)$ of system (2.2).

Contents

Slow-fast normal form

To obtain

- the first Lyapunov coefficient $\hat{A}$,
- singular Hopf bifurcation curve $h_H(\sqrt{\varepsilon})$,
- and maximal canard curve $h_c(\sqrt{\varepsilon})$,

we derive the slow-fast normal form.

Remark: A singular Hopf bifurcation occurs when the eigenvalues become singular as $\varepsilon \to 0$.

- In the following, we derive the slow-fast normal form near the canard point (x_m, y_m).
- Letting $\mathrm{d}t' = x^3\mathrm{d}t$, $\bar{x} = x - x_m$ and $\bar{y} = y - y_m$ in system (2.2) yields

$$\dot{\bar{x}} = -\bar{y} + \bar{x}^2\left(\frac{K - x_m^3}{Kx_m^3} - \frac{1}{x_m^4}\bar{x} + \frac{1}{x_m^5}\bar{x}^2 + O(\bar{x}^3)\right),$$

$$\dot{\bar{y}} = \frac{\varepsilon}{x_m^2}\left(p_0 + p_1\bar{x} + p_2\bar{x}^2 + y(q_0 + q_1\bar{x} + q_2\bar{y}) + O(|(\bar{x}, \bar{y})|^3)\right), \tag{3.1}$$

where

$$p_0 = y_m\left(1 - hy_m x_m^{-1}\right)\left(x_m^2 + bx_m + 1\right),$$

$$p_1 = x_m^{-2} y_m (2bhx_m y_m + y_m h x_m^2 - bx_m^2 + 3hy_m - 2x_m),$$

$$p_2 = -x_m^{-3} y_m (3bx_m y_m + y_m h x_m^2 - bx_m^2 + 6hy_m - 3x_m),$$

$$q_0 = x_m^{-1}(x_m - 2hy_m)(x_m^2 + bx_m + 1),$$

$$q_1 = x_m^{-2}(4bhx_m y_m + 2y_m x_m^2 - bx_m^2 + 6hy_m - 2x_m),$$

$$q_2 = -hx_m^{-1}(x_m^2 + bx_m + 1).$$

Note that p_0 and p_1 have the relationship

$$p_1 = y_m(b + x_m) + \frac{y_m}{x_m} - \frac{3p_0}{x_m(x_m^2 + bx_m + 1)} - \frac{p_0(x_m + 2b)}{x_m^2 + bx_m + 1}.$$

When $(b, K) \in U$, it is feasible to choose h such that

$$p_0 = y_m(1 - h\frac{y_m}{x_m})(x_m^2 + bx_m + 1) = 0.$$

Then we can choose suitable h such that $|p_0|$ is small enough such that $p_1 > 0$. Set

$$\lambda = -\frac{(K - x_m^3)p_0}{Kx_m p_1^{3/2}},\ \bar{x} = \frac{Kx_m\sqrt{p_1}}{K - x_m^3}u,\ \bar{y} = \frac{Kx_m p_1}{K - x_m^3}v,\ t = \frac{x_m}{\sqrt{p_1}}\tau.$$

System (3.1) can be further written as

$$\begin{aligned} \dot{u} &= -vh_1(u,v,\lambda)+u^2h_2(u,v,\lambda)+\varepsilon h_3(u,v,\lambda), \\ \dot{v} &= \varepsilon\left(uh_4(u,v,\lambda)-\lambda h_5(u,v,\lambda)+vh_6(u,v,\lambda)\right), \end{aligned} \tag{3.2}$$

where (u,v) take values near $(0,0)$ and

$$\begin{aligned} &h_1 = 1;\ h_2 = 1 - \frac{K^2 x_m\sqrt{p_1}}{(K-x_m^3)^2}u + \frac{K^3x_m^2p_1}{(K-x_m^3)^3}u^2 + O(|u|^3); \\ &h_3 = 0;\ h_4 = 1 + \frac{p_2Kx_m^2}{\sqrt{p_1}(K-x_m^3)}u + O(|u|^2); \\ &h_5 = 1;\ h_6 = \frac{q_0}{x_m\sqrt{p_1}} + q_1\frac{Kx_m}{K-x_m^3}u + q_2\frac{K\sqrt{p_1}}{K-x_m^3}v + O(|(u,v)|^2). \end{aligned}$$

Remark: $h_3 = O(u,v,\lambda,\varepsilon)$, $h_j = 1 + O(u,v,\lambda,\varepsilon),\ j = 1,2,4,5.$

Based mostly on Krupa and Szmolyan [SIMA, 2001] and [JDE, 2001], we obtain

$$\begin{aligned}
\hat{A} =& (x_m y_m (x_m^2 + b x_m + 1))^{-\frac{1}{2}} (K - x_m^3)^{-2} \hat{A}_1, \\
h_H(\sqrt{\varepsilon}) =& \frac{x_m}{y_m} \left(1 + \frac{K x_m^{3/2} (y_m (b + x_m) + \frac{y_m}{x_m})^{3/2}}{2 y_m^{3/2} (K - x_m^3)(x_m^2 + b x_m + 1)^{1/2}} \varepsilon + O(\varepsilon^{3/2}) \right), \\
h_c(\sqrt{\varepsilon}) =& \frac{x_m}{y_m} \left(1 + \frac{(\frac{1}{2}(\frac{x_m^2 + b x_m + 1}{x_m y_m})^{1/2} - \frac{\hat{A}}{8}) K x_m^2 (y_m (b + x_m) + \frac{y_m}{x_m})^{3/2}}{(K - x_m^3) y_m (x_m^2 + b x_m + 1)} \varepsilon + O(\varepsilon^{3/2}) \right),
\end{aligned} \tag{3.3}$$

with

$$\begin{aligned}
\hat{A}_1 =& 2 \left(K - x_m^3\right)^2 \left(x_m^2 + b x_m + 1\right) \\
& + K x_m y_m \left(\left(b x_m - x_m^2 + 3 \right) K - 4 b x_m^4 - 2 x_m^5 - 6 x_m^3 \right)
\end{aligned} \tag{3.4}$$

Contents

When system (2.2) has only one positive equilibria, There are five distinguished cases to be considered as shown in Fig. 4.1.

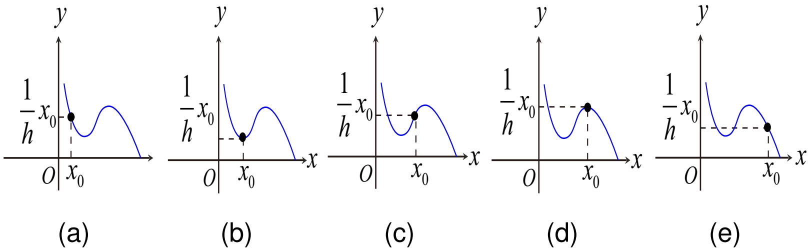

Figure 4.1: Five cases: (a) $x_0 < x_m$, (b) $x_0 = x_m$, (c) $x_m < x_0 < x_M$, (d) $x_0 = x_M$, (e) $x_0 > x_M$.

Cases (d) and (e) in Fig.4.1 could be investigated in the same way as the cases (b) and (a) respectively.

Theorem 4.1 (JDE 2019, Wang and Z.)

If $(K, b, h) \in S_1$ *and the unique positive equilibrium* (x_0, y_0) *lies on the normally hyperbolic attracting critical manifold* C_0^l*, then* (x_0, y_0) *is a global attractor for system* (2.2) *in the interior of the first quadrant.*

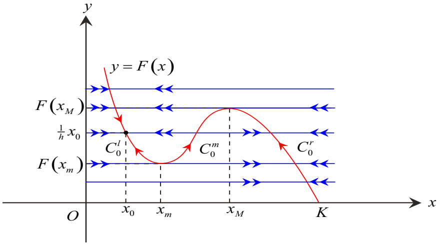

Figure 4.2: Dynamics of the limiting systems for $x_0 < x_m$.

Outline of the proof:

- The line $x = x_m$ divides the interior of the first quadrant into two disjoint regions which we label (from left to right) R_1 and R_2.
- Construct a Dulac function

$$D(x,y) = (x^2 + bx + 1)x^{-2}y^{-2}, \quad (x,y) \in R_1.$$

  From Dulac's criterion, we can conclude that system (2.2) has no closed orbits lying entirely in R_1.
- (x_M, y_M) is a jump point. Trajectory starting at a point in R_2 must eventually cross the line $x = x_m$, and it has (x_0, y_0) as its ω limit.

Example 1

Set $\varepsilon = 0.01$, $K = 3$, $b = -9/5$ and $h = 1/3$. Fig. 4.3 (a) shows some typical orbits of system (2.2), and the behavior of the prey and the predator that system (2.2) is modeling in Fig. 4.3 (b).

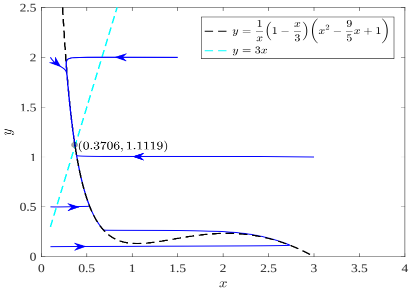

(a)

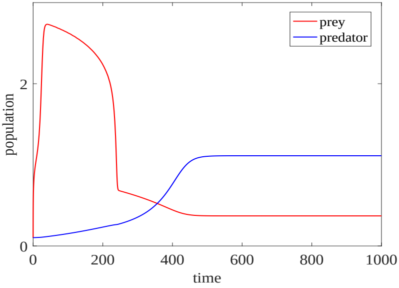

(b)

Figure 4.3: (a) Orbits of system (2.2) starting at points $(0.1, 2)$, $(0.1, 0.5)$, $(0.1, 0.1)$, $(3, 1)$ and $(1.5, 2)$ for $\varepsilon = 0.01$. (b) Behavior of the prey and predator with $x(0) = 0.1$ and $y(0) = 0.1$.

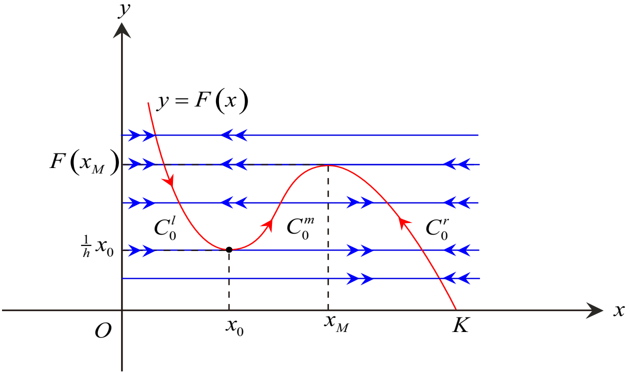

Figure 4.4: Dynamics of the limiting systems for $x_0 = x_m$.

Theorem 4.2 (JDE 2019, Wang and Z.)

Assume that $(K,b,h) \in S_1$, *and that the unique positive equilibrium* (x_0,y_0) *of the slow subsystem of system* (2.2) *coincides with the contact point* (x_m,y_m). *For* $0 < \varepsilon \ll 1$, *the following statements hold for system* (2.2).

(a) *There exists a curve* $h = h_H(\sqrt{\varepsilon})$ *of Hopf bifurcations such that* E *is stable for* $h < h_H(\sqrt{\varepsilon})$. *Moreover, the Hopf bifurcation is nondegenerate when* $A_1 \neq 0$, *and it is supercritical if* $A_1 < 0$ *and subcritical if* $A_1 > 0$. *A canard cycle and a relaxation oscillation coexist when* $A_1 > 0$.

Theorem 4.2 [JDE 2019, Wang and Z.]

(b) Furthermore, there exists a curve $h = h_c(\sqrt{\varepsilon})$, for $\beta \in (0,1)$, the canard explosion occurs when $s \in [\varepsilon^\beta, 2(y_M - y_m) - \varepsilon^\beta]$, where

$$|h(s, \sqrt{\varepsilon}) - h_c(\sqrt{\varepsilon})| \leq e^{-1/\varepsilon^\beta},$$

Example 2

Set $\varepsilon = 0.0001$, $K = 225/32$, $b = 29/32$ and $h = 0.6205$. When h increases, system (2.2) exhibits the supercritical singular Hopf bifurcation, the canard explosion and the relaxation oscillation as shown next.

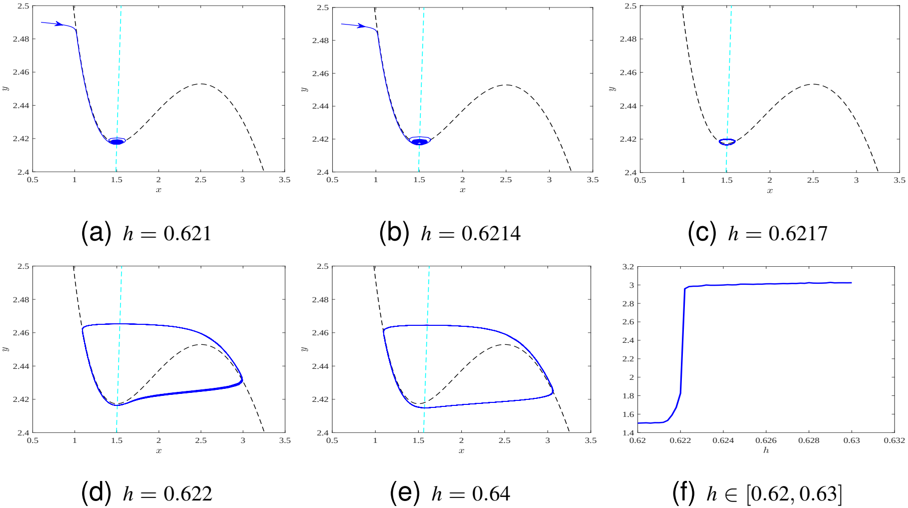

(a) $h = 0.621$ (b) $h = 0.6214$ (c) $h = 0.6217$

(d) $h = 0.622$ (e) $h = 0.64$ (f) $h \in [0.62, 0.63]$

Figure 4.5: (a) A stable focus. (b) A Hopf cycle. (c) Canard cycle without head. (d) Canard cycle with head. (d) Relaxation oscillation. (f) The amplitude (vertical axis) of the limit cycle when h is varied (denote the amplitude by the maximum value of x).

Next, we draw $h_H(\sqrt{\varepsilon})$ and $h_c(\sqrt{\varepsilon})$ in (ε, h) plane for Example 2.

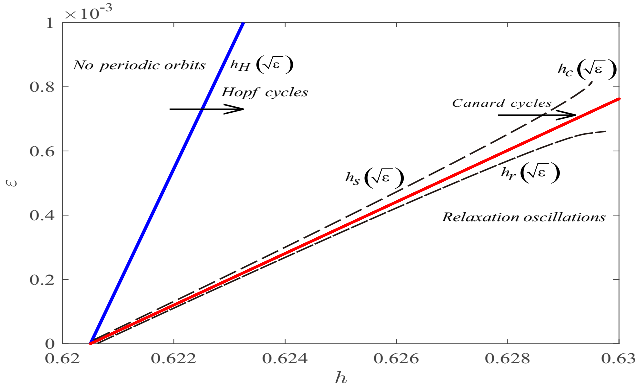

Figure 4.6: Consider $\varepsilon > 0$ fixed. By increasing h, a singular Hopf bifurcation takes place, giving rise to a small stable limit cycle called Hopf cycle with amplitude $O(\varepsilon)$. The amplitude of the Hopf cycle is growing as h increases. When h reaches the dashed line $h_s(\sqrt{\varepsilon})$, the Hopf cycle becomes a canard cycle without head. Along the curve $h_r(\sqrt{\varepsilon})$ the family of canard cycles ends at a relaxation oscillation. The black dashed lines $h_s(\sqrt{\varepsilon})$ and $h_r(\sqrt{\varepsilon})$ mark the beginning and ending of the canard explosion. Furthermore, $|h_i(\sqrt{\varepsilon}) - h_c(\sqrt{\varepsilon})| = O(\mathrm{e}^{-K_0/\varepsilon})$, $i = s, r$, for some $K_0 > 0$ as $\varepsilon \to 0$.

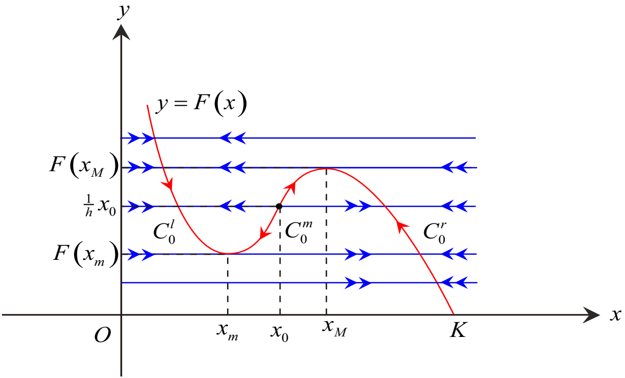

Figure 4.7: The dynamics of limiting systems for $x_m < x_0 < x_M$.

back

Theorem 4.3 (JDE 2019, Wang and Z.)

Assume that $(K, b, h) \in S_1$ *and* x_0 *lies on the normally hyperbolic repelling critical submanifold* C_0^m. *Then for each fixed* $\varepsilon > 0$ *sufficiently small,*

- (a) *system* (2.2) *has a unique limit cycle, say* γ_ε, *which is located in a small tubular neighborhood of the common slow-fast cycle.*
- (b) *Furthermore,* γ_ε *converges to* γ *in the Hausdorff distance as* $\varepsilon \to 0$.

back

Sketch of the proof:

- The unique positive equilibrium (x_0, y_0) of the slow subsystem is an unstable singular node,
- and the critical submanifold C_0^m is normally hyperbolic repelling, see Fig.4.7.
- The two contact points (x_m, y_m) and (x_M, y_M) are both jump points.

- Take a small horizontal section Δ transversal to C_0^l, and choose any two trajectories Γ_ε^1 and Γ_ε^2 of system (2.2) starting on Δ.
- For $\varepsilon > 0$ sufficiently small, it follows from Fenichel's theory that Γ_ε^1 and Γ_ε^2 are attracted to C_ε^l with exponential rate $O(e^{-1/\varepsilon})$.
- Theorem 2.1 in Krupa & Szmolyan [SIMA, 2001] shows that Γ_ε^1 and Γ_ε^2 pass by the jump point (x_m, y_m) contracting exponentially toward each other until they reach a neighborhood of C_0^r.
- Then Γ_ε^1 and Γ_ε^2 are attracted toward C_ε^r with exponentially small rate, and pass by the jump point (x_M, y_M) once more with exponentially small attracting rate, and finally they return to Δ.

- Following the positive orbits of system (2.2) starting on Δ, we can get an attracting map $\Theta : \Delta \to \Delta$ with an exponential small contracting rate $O(e^{-1/\varepsilon})$.
- The contraction mapping theorem verifies that Θ has a unique fixed point on Δ. Consequently, system (2.2) for $0 < \varepsilon \ll 1$ has a unique limit cycle.

Example 3

The relaxation oscillation for system (2.2) when $\varepsilon = 0.0001$, $K = 225/32$, $b = 29/32$ and $h = 14400/17549$.

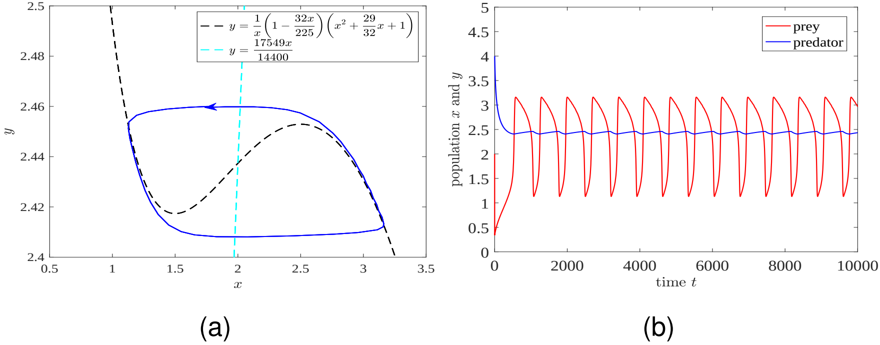

Figure 4.8: (a) The relaxation oscillation for system (2.2). (b) The behavior of x and y depending on time t.

Contents

Assume that $(K, b, h) \in S_2$ and $x_1 < x_2$. Then the locations of the two equilibria can be distinguished into next six cases, where in (a), (b) and (c) $E_2(x_2, y_2)$ is degenerate, whereas in (d), (e) and (f) $E_1(x_1, y_1)$ is degenerate.

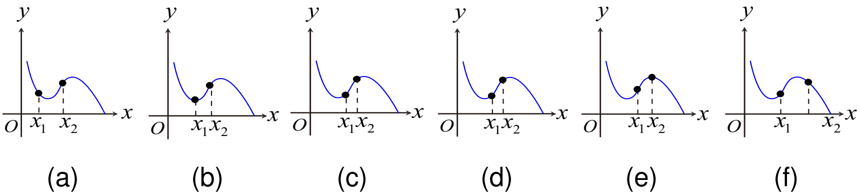

Figure 5.1: (a) $x_1 < x_m < x_2 < x_M$, (b) $x_1 = x_m < x_2 < x_M$, (c) $x_m < x_1 < x_2 < x_M$, (d) $x_m < x_1 < x_2 < x_M$, (e) $x_m < x_1 < x_2 = x_M$, (f) $x_m < x_1 < x_M < x_2$. In cases (a), (b) and (c), $y = F(x)$ is tangent to $y = h^{-1}x$ at $(x_2, F(x_2))$. In cases (d), (e) and (f), $y = F(x)$ is tangent to $y = h^{-1}x$ at $(x_1, F(x_1))$.

back

- Since the cases (d), (e) and (f) in 5.1 can be investigated in the completely same way as the cases (c), (b) and (a), respectively,
- we consider only the first three cases, where E_2 is a degenerate equilibrium.
- Set $H_1 := -10hx_2^3 + 6((K-b)h-K)x_2^2 + 3(Kb-1)hx_2 + Kh$, where
  - $x_2 = -\frac{1}{3}(K/h+b-K) + \frac{1}{3}\sqrt{A}$ in (a), (b) and (c),
  - $x_2 = -\frac{1}{3}(K/h+b-K) - \frac{1}{3}\sqrt{A}$ in (d), (e) and (f).

back

Lemma 5.1

For system (2.2)*, if* $H_1 \neq 0$*, then* E_2 *is a saddle-node, and its local structure is shown in Fig.5.2, where* L^l *and* L^r *are the two branches of the unstable manifold associated to the positive eigenvalue.*

Proof: The proof follows from some calculations of normal form near a saddle-node.

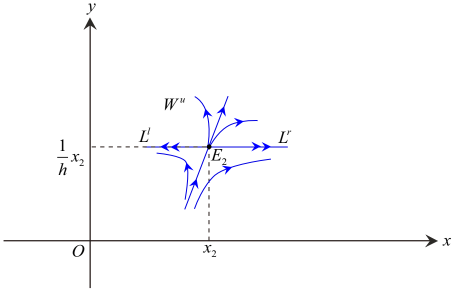

Figure 5.2: Local structure of the saddle-node E_2.

Case (a): Heteroclinic orbits

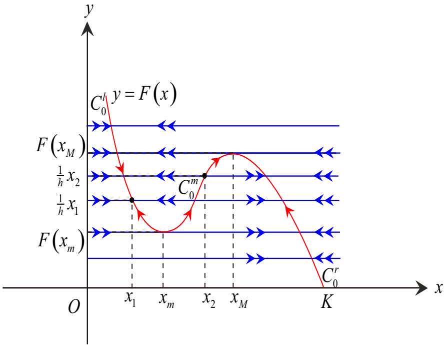

Figure 5.3: The dynamics of limiting systems for $0 < x_1 < x_m < x_2 < x_M$.

back

Theorem 5.1 (JDE 2019, Wang and Z.)

Assume $(K,b,h) \in S_2$ *and* $0 < x_1 < x_m < x_2 < x_M$. *For* $0 < \varepsilon \ll 1$, *the following statements hold.*

- (a) *System* (2.2) *has neither canard cycle nor relaxation oscillation.*
- (b) *If* $H_1 \neq 0$, *system* (2.2) *has infinitely many heteroclinic orbits connecting* E_1 *and* E_2.

Outline of the proof:

- System (2.2) has neither canard points nor slow-fast cycles.
- (x_M, y_M) is a jump point.
- Fenichel's theory.

back

Example 4

Set $\varepsilon = 0.001$, $K = 10$, $b = -9/5$ and $h = 2.7061$. Then system (2.2) has two positive equilibrium: a local stable node $E_1(x_1, y_1) = (0.7369, 0.2723)$ and a degenerate equilibrium $E_2(3.6839, 1.3613)$.

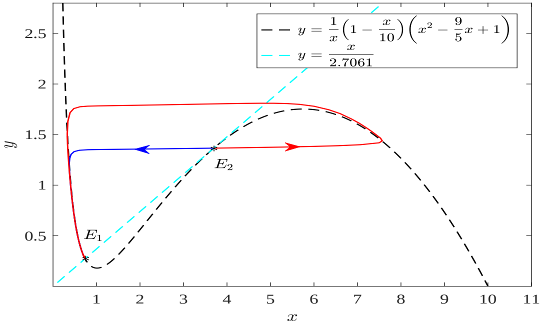

Figure 5.4: Two typical heteroclinic orbits connecting the equilibria E_1 and E_2 for the numerical example.

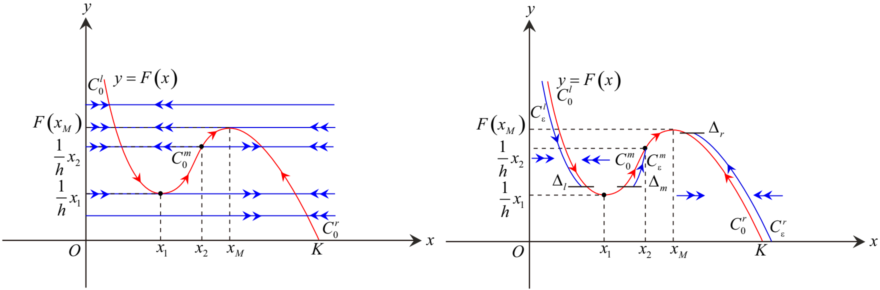

(a) (b)

Figure 5.5: (a) The dynamics of the limiting systems for $x_1 = x_m < x_2 < x_M$. (b) A schematic diagram of the proof of Theorem 5.2: C_ε^l, C_ε^m and C_ε^r are slow manifolds. Δ_l, Δ_m and Δ_r are three horizontal sections.

back

Theorem 5.2 (JDE 2019, Wang and Z.)

Assume $(K,b,h) \in S_3$, $H_1 \neq 0$ *and* $0 < x_1 = x_m < x_2 < x_M < K$. *Then for* $0 < \varepsilon \ll 1$,

(a) *there exists a continuous function* $h = h_c(\sqrt{\varepsilon})$ *such that system* (2.2) *has a unique orbit homoclinic to the saddle-node* $E_2(x_2, y_2)$ *if and only if* $h = h_c(\sqrt{\varepsilon})$.

(b) *Furthermore, if it is the case, system* (2.2) *has a limit cycle* Γ_ε, *which approaches either to the slow-fast cycle without head Fig. 1.2* (c) *or to the slow-fast cycle with head Fig. 1.2* (e).

back

Sketch of the proof:

Preparation:

- By Fenichel's theory, the compact critical submanifolds C_0^l, C_0^m and C_0^r perturb to the nearby slow submanifolds C_ε^l, C_ε^m and C_ε^r, respectively.

- Consider the slow manifold C_ε^l as a example. C_ε^l is not unique. All slow manifolds lie at a Hausdorff distance $O(\mathrm{e}^{-K/\varepsilon})$ from each other for some $K > 0$, $K = O(1)$.

back

- By Theorem 2.1 of Krupa $\&$ Szmolyan [SIMA, 2001], two orbits starting on Δ^r pass by the jump point (x_M, y_M) contracting exponentially toward each other and follow approximately a layer of the fast subsystem to a neighborhood of C_ε^l.
- Let $\gamma^{1,2}$ be two orbits emanating from the infinitely many center manifolds of the saddle-node E_2. $\gamma^{1,2}$ will finally attracted (with exponential rate $O(\mathrm{e}^{-1/\varepsilon})$) to C_ε^l.

back

Having the above preparation, we can prove the existence and uniqueness of the homoclinic orbit to the saddle-node E_2.

- Recall that the positive equilibria of system (2.2) coincide with the positive equilibria of the slow subsystem, and that E_2 is a saddle-node.

- The unique stable branch of the center manifolds of E_2 must coincide with one of the slow manifolds, saying C_ε^{m*}, bifurcating from C_0^m and with E_2 located on it.

- Thus, there is only one way that the homoclinic orbit (if exists) can return to the saddle-node. However, it could leave the saddle-node along any one (priori) of the infinitely many orbits composing the unstable set W^u of E_2.

- Now turn to the any chosen orbit γ emanating from E_2, it is rapidly attracted to a $O(\varepsilon)$ neighborhood of C_0^l,

- and then follow C_0^l positively, during this last period γ is a slow manifold bifurcating from the critical manifold C_0^l, and becomes a C_ε^{l*}.

- Next we analyze the conditions such that C_ε^{l*} and C_ε^{m*} could connect.

back

- Theorem 3.2 in Krupa $\&$ Szmolyan [JDE, 2001], shows that a connection from C_{ε}^{l*} to C_{ε}^{m*} exists if and only if $h = h_c(\sqrt{\varepsilon})$

This proves that under the condition $h = h_c(\sqrt{\varepsilon})$ the orbit γ is homoclinic to E_2.

Next, we prove the second part of the theorem.

- We define the Poincaré map on Δ_l in 5.5 (b) for system (2.2).
- For any orbit starting on Δ_l and located outside the homoclinic orbit γ, it first follows C_0^l until arriving at a small neighborhood of the canard point (x_m, y_m),
- and passes it in the way either flighting to the vicinity of C_0^r or following C_0^m a while and then flighting to C_0^r (this fact holds because of the existence of the homoclinic orbit γ at E_2),

◂ back

- then it follows C_0^r until arriving at a small vicinity of the jump point (x_M, y_M), and jumps from this point to the vicinity of C_0^l,
- next it follows C_0^l again and arrives at Δ_l.
- The Poincaré map is a contraction.
- Hence, it follows from the contraction map theorem that the Poincaré map has a unique fixed point on Δ_l, which provides a limit cycle of system (2.2) for $\varepsilon > 0$ sufficiently small.

back

Case (c): Relaxation oscillations

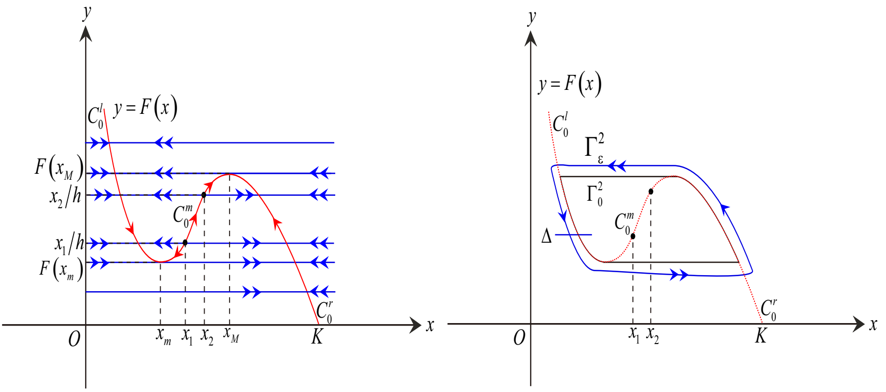

(a) (b)

Figure 5.6: (a) The dynamics of limiting systems for $x_m < x_1 < x_2 < x_M$. (b) The sketch of the relaxation oscillation of system (2.2) for $x_m < x_1 < x_2 < x_M$.

Theorem 5.3 (JDE 2019, Wang and Z.)

Assume that $(K, b, h) \in S_3$ *and* x_1 *and* x_2 *lie on the normally hyperbolic repelling critical submanifold* C_0^m. *Then for each fixed* $\varepsilon > 0$ *sufficiently small,*

(a) *system* (2.2) *has a unique limit cycle, say* Γ_ε^2, *which is a relaxation oscillation and is located in a small tubular neighborhood of the common slow-fast cycle* Γ_0^2.

(b) *Furthermore,* Γ_ε^2 *converges to* Γ_0^2 *in the hausdorff distance as* $\varepsilon \to 0$.

Outline of the proof:

- The two contact points (x_m, y_m) and (x_M, y_M) are both jump points.
- Construct a contraction map.

Contents

- In this section we assume that the parameters $(K, b, h) \in S_3$.
- Then system (2.2) has exactly three positive equilibria E_1, E_2 and E_3.
- There are nine different cases to be considered, which are:
  - (a) $x_1 < x_m < x_2 < x_M < x_3$, (b) $x_1 < x_m < x_2 < x_3 < x_M$,
  - (c) $x_m < x_1 < x_2 < x_M < x_3$, (d) $x_m < x_1 < x_2 < x_3 < x_M$,
  - (e) $x_1 = x_m < x_2 < x_3 < x_M$, (f) $x_m < x_1 < x_2 < x_3 = x_M$,
  - (g) $x_1 = x_m < x_2 < x_M < x_3$, (h) $x_1 < x_m < x_2 < x_3 = x_M$
  - (i) $x_1 = x_m < x_2 < x_3 = x_M$.

By Fenichel's theory and Fig. 6.1 (a) one gets that system (2.2) has E_1 and E_3 as stable nodes, and E_2 as a saddle.

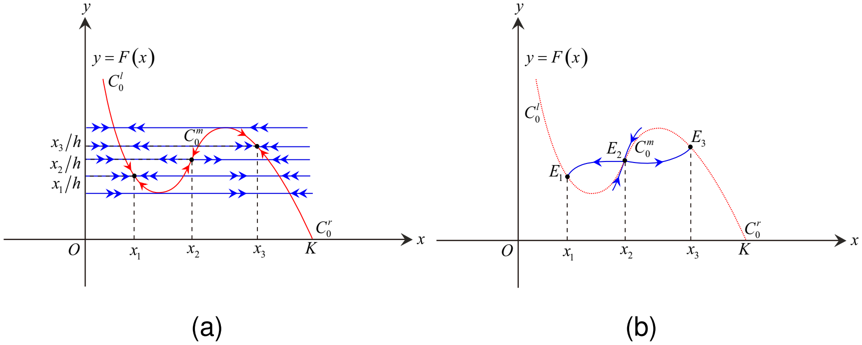

Figure 6.1: (a) The dynamics of the limiting systems for $x_1 < x_m < x_2 < x_M < x_3$. (b) A schematic diagram of heteroclinic orbits connecting equilibria E_1 and E_2, and E_2 and E_3 of system (2.2).

Theorem 6.1

Assume $(K, b, h) \in S_3$*, and* $x_1 < x_m < x_2 < x_M < x_3$*.*

(a) *For* $0 < \varepsilon \ll 1$*, system* (2.2) *has heteroclinic orbits connecting the equilibria* E_1 *and* E_2*, and* E_2 *and* E_3*,*

(b) *and has no periodic orbits in the first quadrant.*

Outline of the proof:

- Fenichel's theory.
- System has neither canard points nor slow-fast cycles.

Example 5

Set $\varepsilon = 0.001$, $K = 10$, $b = -9/5$ and $h = 4$. Fig.6.2 shows that heteroclinic orbits connecting the equilibria E_1 and E_2, and E_2 and E_3.

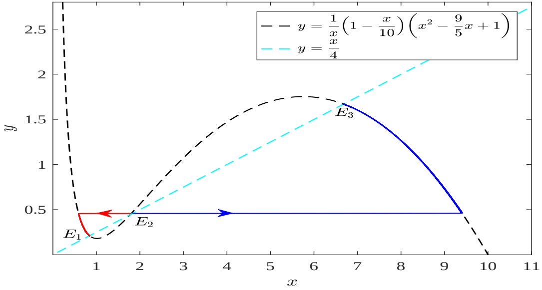

Figure 6.2: A numerical example showing the existence of the heteroclinic orbits.

Case (b): Heteroclinic orbits

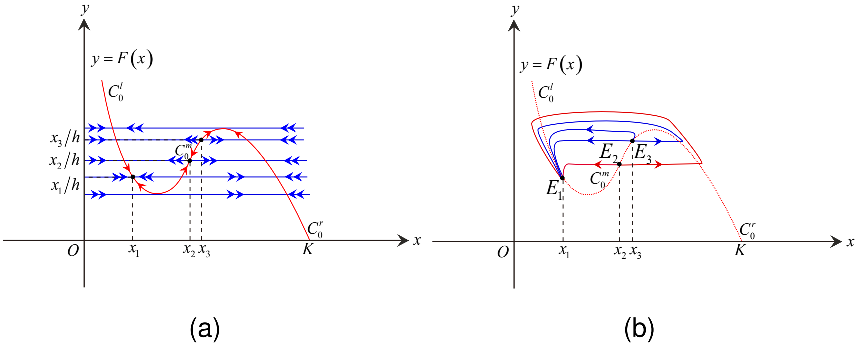

Figure 6.3: (a) The dynamics of the limiting systems for $x_1 < x_m < x_2 < x_3 < x_M$. (b) A schematic diagram of heteroclinic orbits of system (2.2): two heteroclinic orbits (solid red) connecting equilibria E_1 and E_2 and three heteroclinic orbits (solid blue) connecting equilibria E_1 and E_3.

Theorem 6.2

Assume $(K, b, h) \in S_3$, *and* $x_1 < x_m < x_2 < x_3 < x_M$.

(a) *For* $0 < \varepsilon \ll 1$, *system* (2.2) *has two heteroclinic orbits connecting the equilibria* E_1 *and* E_2,

(b) *has infinitely many heteroclinic orbits connecting* E_1 *and* E_3,

(c) *and has no periodic orbits in the first quadrant.*

Example 6

Set $\varepsilon = 0.001$, $K = 10$, $b = -9/5$ and $h = 3$. Fig. 6.4 shows that heteroclinic orbits connecting the equilibria E_1 and E_2, and E_1 and E_3.

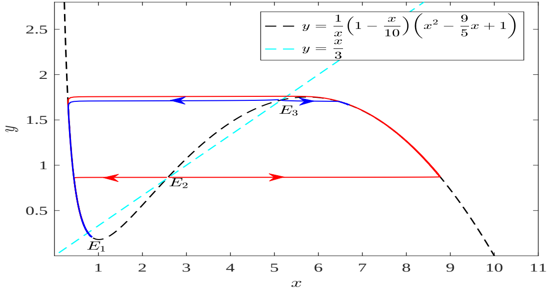

Figure 6.4: A numerical example.

- Case (c) is similar to the case (b), and so the detail statements are omitted.

- By Fenichel's theory we know E_1 and E_3 are unstable nodes and E_2 is a saddle .

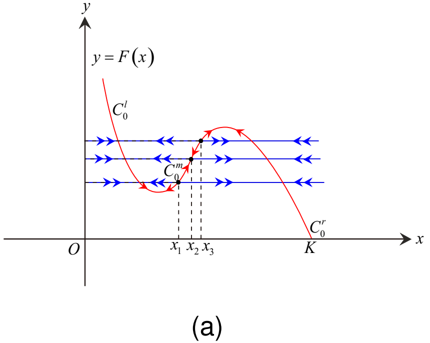

Figure 6.5: (a) The dynamics of the limiting systems for $x_m < x_1 < x_2 < x_3 < x_M$. (b) A schematic diagram of the relaxation oscillation for $x_m < x_1 < x_2 < x_3 < x_M$.

Theorem 6.3

Let U be a small tubular neighborhood of the common slow-fast cycle Γ_0. Then for each fixed $\varepsilon > 0$ sufficiently small, there exists a unique relaxation oscillation $\Gamma_\varepsilon^3 \subset U$, which is the only limit cycle of system (2.2) *and converges to Γ_0 in the Hausdorff distance as $\varepsilon \to 0$.*

Example 7

Set $\varepsilon = 0.001$, $K = 2.9153$, $b = -1.8135$ and $h = 9$. Fig. 6.6 shows that there exists a relaxation oscillation for system (2.2).

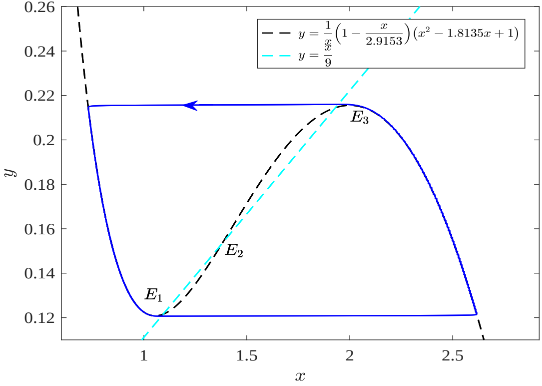

Figure 6.6: A relaxation oscillation for $x_m < x_1 < x_2 < x_3 < x_M$ generated by a numerical example.

By Fenichel's theory we know E_2 is a saddle and E_3 is an unstable node of system (2.2).

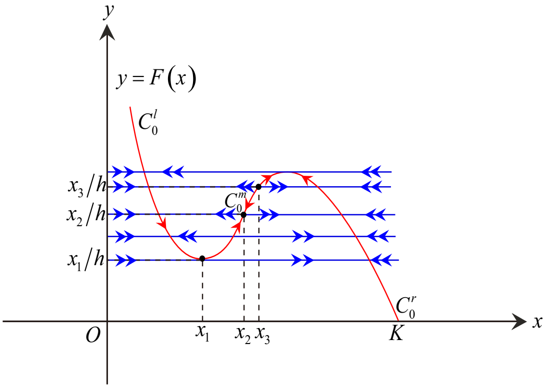

Figure 6.7: The dynamics of the limiting systems for $x_m = x_1 < x_2 < x_3 < x_M$.

Next result shows the existence of “small” or “big” homoclinic orbits , where the “small” homoclinic orbit is the one passing only one contact point; whereas the “big” homoclinic orbit is the one passing the two contact points, see Fig. 6.8

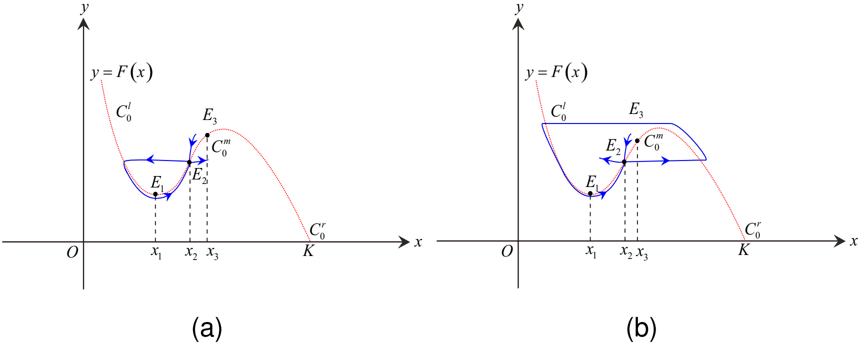

Figure 6.8: (a) A “small” homoclinic orbit. (b) A “big” homoclinic orbit.

Theorem 6.4

Assume $(K, b, h) \in S_3$, *and* $0 < x_1 = x_m < x_2 < x_3 < x_M < K$. *Then for* $0 < \varepsilon \ll 1$, *the following statements hold.*

(a) *There exists a continuous function* $h_c(\sqrt{\varepsilon})$ *having the expression* (3.3) *such that system* (2.2) *has an orbit homoclinic to the saddle* E_2, *which is either small or big, if and only if* $h = h_c(\sqrt{\varepsilon})$. *Depending on the different choice of* $h_c(\sqrt{\varepsilon})$, *both of the small and big ones could appear but not simultaneously.*

Theorem 6.4

(b) When varying h from $h_c(\sqrt{\varepsilon})$ sufficiently small, the homoclinic orbit bifurcates a unique canard cycle without head when it is small, or a unique canard cycle with head if it is big. Furthermore, the unique canard cycle is unstable and exists for $0 < h_c(\sqrt{\varepsilon}) - h \ll 1$.

Geometrical interpretation of the proof:

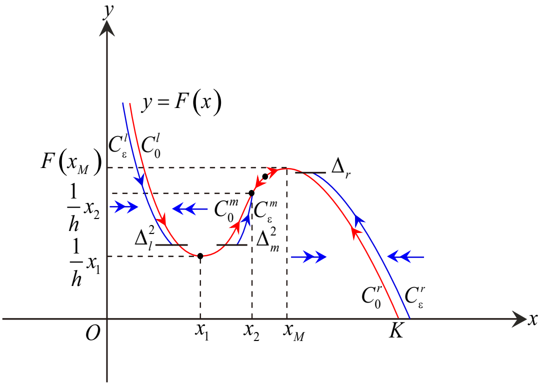

Figure 6.9: A schematic diagram for the proof of Theorem 6.4.

- Case (f) is similar to the case (e), and so the detail statements are omitted.

System (2.2) for $0 < \varepsilon \ll 1$ has E_2 as a saddle and E_3 as a stable node respectively, whereas E_1 is a canard point.

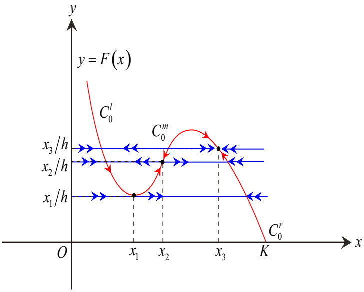

(a)

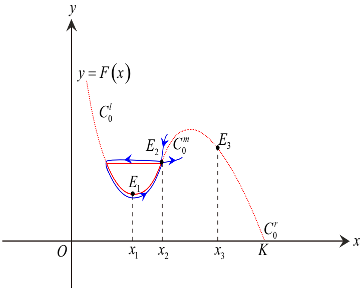

(b)

Figure 6.10: (a) The dynamics of the limiting system for $x_1 = x_m < x_2 < x_M < x_3$. (b) A small homoclinic orbit.

Next result shows the existence of small homoclinic orbit and canard cycle without head.

Theorem 6.5

Assume $(K, b, h) \in S_3$, *and* $0 < x_1 = x_m < x_2 < x_M < x_3 < K$. *Then for* $0 < \varepsilon \ll 1$, *the following statements hold.*

(a) *There exists a continuous function* $h_c(\sqrt{\varepsilon})$ *having the expression* (3.3) *such that system* (2.2) *has an orbit homoclinic to the saddle* $E_2(x_2, y_2)$ *if and only if* $h = h_c(\sqrt{\varepsilon})$.

(b) *When varying* h *from* $h_c(\sqrt{\varepsilon})$ *sufficiently small, the homoclinic orbit bifurcates to a unique canard cycle without head. Furthermore, the unique canard cycle is unstable and exists for* $0 < h_c(\sqrt{\varepsilon}) - h \ll 1$.

- Case (h) is similar to the case (b), and so the detail statements are omitted.

Now E_2 is a saddle for system (2.2), and E_1 and E_3 are both located at the contact points of the critical manifold.

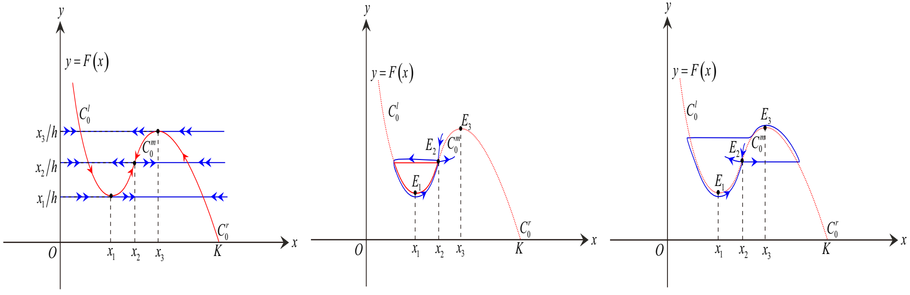

(a) (b) (c)

Figure 6.11: (a) The dynamics of limiting systems for $x_1 = x_m < x_2 < x_3 = x_M$. (b) A small homoclinic orbit. (c) A big homoclinic orbit.

Next result shows the existence of small or big homoclinic orbit and canard cycle without head.

Theorem 6.6

Assume $(K, b, h) \in S_3$ *and* $x_1 = x_m < x_2 < x_M = x_3$. *Then for* $0 < \varepsilon \ll 1$, *the following statements hold.*

(a) *There exists a continuous function* $h_c(\sqrt{\varepsilon})$ *of form* (7) *such that system* (2.2) *has a small homoclinic orbit if and only if* $h = h_c(\sqrt{\varepsilon})$.

(b) *Furthermore, a unique canard cycle without head bifurcates from the homoclinic orbit when* h *varies slightly from* $h = h_c(\sqrt{\varepsilon})$. *The unique canard cycle is unstable and exists for* $0 < h_c(\sqrt{\varepsilon}) - h \ll 1$.

Theorem 6.6

(c) Assume that E_3 always coincides with the contact point (x_M, y_M) when h varies slightly from $h = h_c(\sqrt{\varepsilon})$. Then there exists a continuous function $h_c(\sqrt{\varepsilon})$ of form (7) such that system (2.2) has a big homoclinic orbit if and only if $h = h_c(\sqrt{\varepsilon})$.

(d) A unique canard cycle with head bifurcates from the big homoclinic orbit when λ varies slightly from $h = h_c(\sqrt{\varepsilon})$. The unique canard cycle is unstable and exists for $0 < h_c(\sqrt{\varepsilon}) - h \ll 1$.

Contents

Recall that in the interior of the first quadrant system (2.2) is smoothly equivalent to the system of the form

$$\begin{aligned} \frac{\mathrm{d}x}{\mathrm{d}t} &= \frac{1}{x}\left(1-\frac{x}{K}\right)(x^2+bx+1)-y \equiv f(x,y,\eta), \\ \frac{\mathrm{d}y}{\mathrm{d}t} &= \varepsilon y \frac{1}{x^2}\left(1-h\frac{y}{x}\right)(x^2+bx+1) \equiv \varepsilon g(x,y,\eta), \end{aligned} \tag{7.1}$$

with $\eta = (b, K, h)$, and $(b, K) \in U$. We have clearly the next result.

Lemma 7.1

Assume that $(x_j, F(x_j))$ is a canard point of system (7.1), $j \in \{m,\ M\}$. *Then for any $(b, K) \in U$ system* (7.1) *for $\varepsilon = 0$ could have a slow-fast cycle passing $(x_j, F(x_j))$.*

Next, according to the analysis on the number, types and relative locations of positive equilibria of the slow subsystem of system (7.1), we can provide a complete list of slow-fast cycles, which are illustrated in Figs. 7.1, 7.2 and 7.3 as a schematic view.

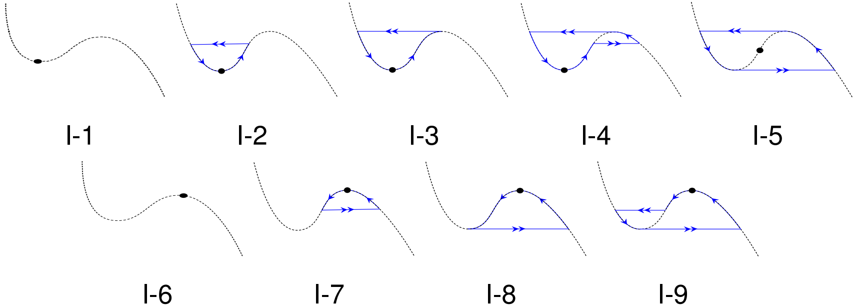

Figure 7.1: Slow-fast cycles when system (7.1) (or system (2.2)) has one positive equilibrium (black dot).

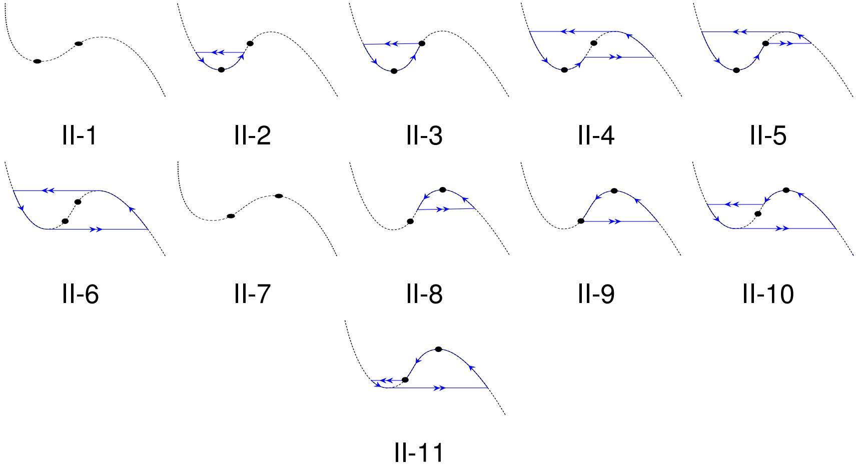

Figure 7.2: Slow-fast cycles when system (7.1) (or system (2.2)) has two positive equilibria (black dots) where one equilibrium is a saddle-node.

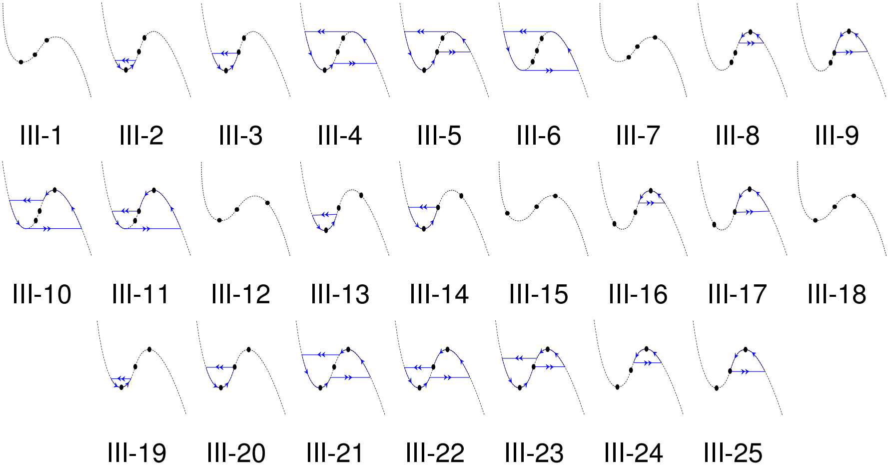

Figure 7.3: Slow-fast cycles when system (7.1) (or system (2.2)) has three positive equilibria (black dots) where equilibrium E_2 is a saddle.

Let Γ_s^f be the set of all slow-fast cycles shown in Figs. 7.1, 7.2 and 7.3. We can express Γ_s^f as the disjoint union of the next subsets:

(a) Small cycles: $\Gamma_{\bullet}$:= {(I-1), (I-6), (II-1), (II-7), (III-1), (III-7), (III-12), (III-15), (III-18)}.

(b) Slow-fast cycles without head: Γ_{U}^m := {(I-2), (II-2), (II-3), (III-2), (III-3), (III-13), (III-14), (III-19), (III-20)}, Γ_{U}^M := {(I-7), (II-8), (II-9), (III-8), (III-9), (III-16), (III-17), (III-24), (III-25)}.

(c) Slow-fast cycles with head: Γ_{S}^m := {(I-4), (II-4), (II-5), (III-4), (III-5)}, Γ_{S}^M := { (I-9), (II-10), (II-11), (III-10), (III-11)}, Γ_{S}:={(III-21), (III-22), (III-23)}.

(d) Transitory slow-fast cycles: Γ_{U}^T :={(I-3), (I-8)}.

(e) Common slow-fast cycles: Γ_{C}:={(I-5), (II-6), (III-6)}.

- Since the proofs on the cyclicity of the slow-fast cycles in Γ_U^m and in Γ_U^M, in Γ_S^m and in Γ_S^M, and $(\text{I-}3)$ and $(\text{I-}8)$ in Γ_U^T respectively are very similar in most cases,
- in what follows we only study the limit cycles bifurcated from the formers in each of pairs, and the ones in latter which are different.
- For doing so, we first define the SDI along the slow-fast cycles in $\Gamma_{\rm U}^m$ and $\Gamma_{\rm S}^m$, respectively.
- Denote by $X_{\varepsilon,\eta}$ the vector field associated to system (7.1), with $\eta = (K, b, h)$.

- Let (x_m, y_m) be a non-degenerate canard point and (x_M, y_M) be a non-degenerate jump point.
- Hence there exists a solution $x_0(t)$ of the slow subsystem connecting C_0^l and C_0^m.
- There is a solution $\hat{x}_0(t)$ of the slow subsystem, which corresponds to the slow flow on C_0^r.

- Let $t_l(s) \leq 0 \leq t_m(s)$ be such that

$$F(x_0(t_l(s))) = F(x_0(t_m(s))) = y_m + s,$$

and let $t_r(s)$ be defined by

$$F(\hat{x}_0(t_r(s))) = y_m + s.$$

Next, we defined the so-called slow divergence integral.

- For the slow-fast cycle in $\Gamma_U^m \cup \{(\text{I-}3)\}$, define the function $I(s,\eta_0)$ as

$$I(s,\eta_0)=\int_{t_l(s)}^{t_m(s)}\frac{\partial f}{\partial x}(x_0(t),F(x_0(t)),\eta_0)\mathrm{d}t,\ \ s\in[0,s_0], \qquad (7.2)$$

  where $s_0=y_M-y_m$.

- For the slow-fast cycle in Γ_S^m, define the function $I(s,\eta_0)$ as

$$\begin{aligned}I(s,\eta_0)=&\int_{t_l(s_0)}^{t_m(s)}\frac{\partial f}{\partial x}(x_0(t),F(x_0(t)),\eta_0)\mathrm{d}t\\&+\int_{t_r(s)}^{T}\frac{\partial f}{\partial x}(\hat{x}_0(t),F(\hat{x}_0(t)),\eta_0)\mathrm{d}t,\ \ s\in[0,s_0].\end{aligned} \qquad (7.3)$$

The above two integrals $I(s,\eta_0)$ are called slow divergence integrals (SDIs).

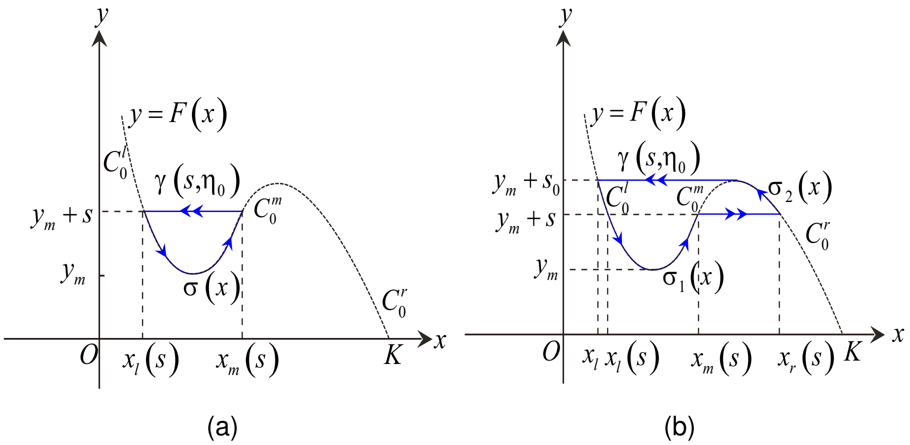

Figure 7.4: Illustration for the slow divergence integral when (x_m, y_m) is a canard point. (a) A slow-fast cycle $\gamma(s, \eta_0)$ without head (blue curve). (b) A slow-fast cycle $\gamma(s, \eta_0)$ with head (blue curve).

Making the change of integration variable from t to x in (7.2) and (7.3) yields

- $$I(s,\eta_0)=\int_{x_l(s)}^{x_m(s)}\frac{\partial f}{\partial x}(x,F(x),\eta_0)\frac{F'(x)}{g(x,F(x),\eta_0)}\mathrm{d}x,\quad s\in[0,s_0],\tag{7.4}$$

- $$\begin{aligned}I(s,\eta_0)=&\int_{x_l}^{x_m(s)}\frac{\partial f}{\partial x}(x,F(x),\eta_0)\frac{F'(x)}{g(x,F(x),\eta_0)}\mathrm{d}x\\&+\int_{x_r(s)}^{x_M}\frac{\partial f}{\partial x}(x,F(x),\eta_0)\frac{F'(x)}{g(x,F(x),\eta_0)}\mathrm{d}x,\ \ s\in[0,s_0].\end{aligned}\tag{7.5}$$

- If the slow-fast cycle has no a head (see 7.4 (a)), for $x \in [x_l, x_m]$, we define $\sigma(x)$ by $F(x) = F(\sigma(x))$. Hence for $x \in [x_l, x_m)$, we have

$$\sigma'(x) = \frac{F'(x)}{F'(\sigma(x))} < 0.$$

- If the slow-fast cycle has a head (see 7.4 (b)), for each $x \in [x_l, x_m]$, we define $\sigma_1(x) \in [x_m, x_M]$ and $\sigma_2(x) \in [x_M, x_r]$ by $F(x) = F(\sigma_j(x)),\ j = 1, 2$. For $x \neq x_m,\ x \neq x_M$ one has

$$\sigma_1^{'}(x) = \frac{F'(x)}{F'(\sigma_1(x))} < 0,\ \sigma_2^{'}(x) = \frac{F'(x)}{F'(\sigma_2(x))} > 0.$$

Let

$$h(x) = \frac{\frac{\partial f}{\partial x}(x, F(x), \eta_0)}{g(x, F(x), \eta_0)} \tag{7.6}$$

and let $x = F^{-1}(y)$ be the single-valued inverse function of $y = F(x)$ for $x \in [x_l, x_m]$. The following results hold.

Lemma 7.2

For $s \in [0, s_0]$, the SDIs (7.4) *and* (7.5) *can be written respectively as*

$$I(s, \eta_0) = \int_{y_m}^{y_m+s} (h(\sigma(x)) - h(x))\Big|_{x=F^{-1}(y)} \mathrm{d}y \tag{7.7}$$

$$I(s, \eta_0) = \int_{y_m}^{y_m+s} (h(\sigma_1) - h(x))\Big|_{x=F^{-1}(y)} \mathrm{d}y + \int_{y_m+s}^{y_M} (h(\sigma_2) - h(x))\Big|_{x=F^{-1}(y)} \mathrm{d}y. \tag{7.8}$$

Now we recall some results developed by De Maesschalck and Dumortier.

[Theorem 1, C. R. Math. Acad. Sci. Paris, 2014]

When $I(s, \eta_0) \neq 0$ for the transitory slow-fast cycle $\gamma(s, \eta_0)$ as shown in Fig. 1.2 (b), system (2.2) has at most one periodic orbit Hausdorff close to $\gamma(s, \eta_0)$ for $0 < \varepsilon \ll 1$. When $I(s, \eta_0) = 0$, there are at most two periodic orbits Hausdorff close to $\gamma(s, \eta_0)$.

Definition 7.1

A slow-fast cycle $\gamma(s, \eta_0)$ is called non-degenerate, if it is not transitory and all of its contact points (fold points) are non-degenerate. Here a *transitory slow-fast cycle* is the one given in Fig.1.2 (b).

[Theorems 2.22, 2.23 and 2.24, Proc. Roy. Soc. E. A, 2008]

If a slow-fast cycle $\gamma(s,\eta_0)$ is non-degenerate as shown in Fig.7.4 (a) or (c), then the following statements hold.

(a) If $I(s,\eta_0) \neq 0$, then $\mathrm{Cycl}(X_{\varepsilon,\eta}, \gamma(s), (0,\eta_0)) \leq 1$. Moreover, if $I(s,\eta_0) < 0$ (or > 0) then the perturbed canard cycle from $\gamma(s,\eta_0)$ is stable (or unstable).

(b) If $I(s,\eta_0) = 0$ and $\dfrac{\partial I}{\partial s}(s,\eta_0) \neq 0$, then $\mathrm{Cycl}(X_{\varepsilon,\eta}, \gamma(s), (0,\eta_0)) \leq 2$.

(c) If $I(s,\eta_0) = 0$ and (s,η_0) is a zero point of $\dfrac{\partial I}{\partial s}$ with multiplicity m, then $\mathrm{Cycl}(X_{\varepsilon,\eta}, \gamma(s), (0,\eta_0)) \leq 2+m$.

[Theorems 2, Indag. Math., 2011]

When $\gamma(s, \eta_0)$ is a common slow-fast cycle as shown in Fig. 1.2 (d), there is a unique hyperbolic periodic orbit Hausdorff close to $\gamma(s, \eta_0)$ for sufficiently small $\varepsilon > 0$.

- Note that each small slow-fast cycle in $\Gamma_{\bullet}$ is in fact a canard point.
- The maximal number of small limit cycles born from a canard point under perturbation is from Hopf bifurcation.
- For $0 < \varepsilon \ll 1$, the coexistence of two limit cycles when system (2.2) has a unique positive equilibrium can be proved by the canard explosion phenomenon,
- the coexistence of Hopf cycle and relaxation oscillation or the canard cycle without head and canard cycle with head.

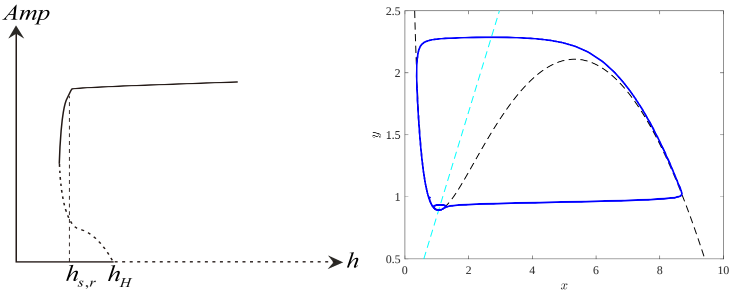

(a) (b)

Figure 7.5: (a) Sketch of the bifurcation diagram corresponding to the subcritical singular Hopf bifurcation for system (2.2). *Amp* denotes the amplitude of the limit cycles. h_s and h_r marking the beginning and the ending of canard explosion. (b) The coexistence of a canard cycle without head and a canard cycle with head when $K = 10, b = -11/10$ in system (2.2).

Proposition 7.1

Assume that $(K, b, h) \in S_1$*, and that the unique positive equilibrium of the slow subsystem of system* (2.2) *coincides with the contact point* (x_m, y_m)*. Let* $\hat{A}_1$ *defined in* (3.3) *be positive. Then for* $0 < \varepsilon \ll 1$*,*

(a) *If* $h > h_H(\varepsilon)$*, system* (2.2) *has a unique stable relaxation oscillation surrounding an unstable equilibrium.*

(b) *If* $h = h_H(\varepsilon)$*, system* (2.2) *exhibits a subcritical singular Hopf bifurcation.*

(c) *If* $h_c(\varepsilon) < h < h_H(\varepsilon)$*, system* (2.2) *has two limit cycles surrounding a stable equilibrium, where the inner cycle is unstable and the outer cycle is stable. More precisely, the two limit cycles either are the small Hopf cycle and the big relaxation oscillation or the canard cycle without head and the canard cycle with head.*

- We have a basic assumption that $b \geq -1$ in the following.
- For system (7.1), the function $h(x)$ defined in (7.6) along the slow-fast cycle has the expression

$$
\begin{aligned}
h(x) &= \frac{F'(x)}{F(x)x^{-2}(1-h_0x^{-1}F(x))(x^2+bx+1)} \\
&= -\frac{Kx^3(2x^3+(b-K)x^2+K)}{(K-x)(x^2+bx+1)^2(Kx^2-h_0(K-x)(x^2+bx+1))}.
\end{aligned}
$$

- First we discuss the cyclicity of the slow-fast cycle $\gamma_{\mathrm{u}}^m(s) \in \Gamma_{\mathrm{U}}^m$,
- According to Lemma 7.2, we need to consider the following SDI

$$I(s,\eta_0) = \int_{y_m}^{y_m+s} (h(\sigma(x)) - h(x))\Big|_{x=F^{-1}(y)} \mathrm{d}y, \quad (b,K) \in U, \quad (7.9)$$

where

  - $\sigma(x) \in (x_m, x_m(s))$ is defined by $F(x) = F(\sigma(x))$ for $x \in (x_l(s), x_m)$.
  - $x = F^{-1}(y)$ is the single-valued inverse function of $y = F(x)$ for $x \in (x_l(s), x_m)$.

- Some calculations show that $h(\sigma(x)) - h(x) < 0$ in (7.9) for $(b, K) \in U$ and $b \geq -1$.

- Next we discuss the slow-fast cycle $\gamma_{\mathrm{u}}^{M}(s) \in \Gamma_{\mathrm{U}}^{M}$,

- the SDI can be written in

$$I(s,\eta_0) = \int_{y_M}^{y_m+s} (h(\sigma_1(x)) - h(\sigma_2(x)))\Big|_{x=F^{-1}(y)} \mathrm{d}y, \quad (b,K) \in U, \tag{7.10}$$

  where
  - $\sigma_1(x) \in (x_m(s), x_M) \subset (x_m, x_M)$ and $\sigma_2(x) \in (x_M, x_r(s)) \subset (x_M, x_r)$ are defined by $F(x) = F(\sigma_1(x)) = F(\sigma_2(x))$ for $x \in (x_l, x_l(s))$.
  - $x = F^{-1}(y)$ is the single-valued inverse function of $y = F(x)$ for $x \in (x_l, x_l(s))$.
- The similar arguments as did for (7.9) show that the slow divergence integral is positive for $(b,K) \in U$ and $b \geq -1$.

Based on the above analysis, we have the following result.

Proposition 7.2

For system (2.2) *with* $0 < \varepsilon \ll 1$, *if* $(b, K) \in U$ *and* $b \geq -1$, *then the cyclicity of the slow-fast cycles without head contained in* $\Gamma_{\mathrm{U}}^{m} \cup \Gamma_{\mathrm{U}}^{M}$ *is at most one. Furthermore, the canard cycles bifurcated from the slow-fast cycles belonging to* Γ_{U}^{m} $($*resp.* $\Gamma_{\mathrm{U}}^{M})$ *are stable* $($*resp. unstable*$)$.

Cyclicity of the slow-fast cycle with head

- We first study the cyclicity of the slow-fast cycle $\gamma_s^m(s) \in \Gamma_S^m$.
- According to Lemma 7.2, we need to consider the SDI

$$I(s,\eta_0) = \int_{y_m}^{y_m+s} (h(\sigma_1(x)) - h(x))\Big|_{x=F^{-1}(y)} \mathrm{d}y + \int_{y_m+s}^{y_M} (h(\sigma_2(x)) - h(x))\Big|_{x=F^{-1}(y)} \mathrm{d}y,$$

where

- $\sigma_1(x) \in (x_m, x_m(s)) \subset (x_m, x_M)$ and $\sigma_2(x) \in (x_M, x_r(s)) \subset (x_M, x_r)$ are defined by $F(x) = F(\sigma_1(x))$ for $x \in (x_l(s), x_m)$ and $F(x) = F(\sigma_2(x))$ for $x \in (x_l, x_l(s))$.
- $x = F^{-1}(y)$ is the single-valued inverse function of $y = F(x)$ for $x \in (x_l, x_m)$.

- Some analysis shows that $I(s, \eta_0)$ is negative for $(b, K) \in U$ and $b \geq -1$.
- Next, we consider the cyclicity of the slow-fast cycle $\gamma_{\rm s}^{M}(s)$ contained in $\Gamma_{\rm S}^{M}$.

- According to 7.2, we need to consider the following SDI

$$
\begin{aligned}
I(s,\eta_0) = &\int_{y_m}^{y_m+s} (h(\sigma_2(x)) - h(x))\Big|_{x=F^{-1}(y)} \mathrm{d}y \\
&+ \int_{y_m+s}^{y_M} (h(\sigma_2(x)) - h(\sigma_1(x)))\Big|_{x=F^{-1}(y)} \mathrm{d}y,
\end{aligned}
\tag{7.11}
$$

where

- $\sigma_1(x) \in (x_m(s), x_M) \subset (x_m, x_M)$ and $\sigma_2(x) \in (x_M, x_r)$ are defined by $F(x) = F(\sigma_1(x)) = F(\sigma_2(x))$ for $x \in (x_l, x_l(s))$ and $F(x) = F(\sigma_2(x))$ for $x \in (x_l(s), x_m)$, respectively.
- $x = F^{-1}(y)$ is the single-valued inverse function of $y = F(x)$ for $x \in (x_l, x_m)$.

- Applying the same arguments as those we did for the slow-fast cycle $\gamma_s^m(s)$, one obtains that $h(\sigma_2(x)) - h(x) < 0$ for $(b, K) \in U$ and $h(\sigma_2(x)) - h(\sigma_1(x)) > 0$ for $(b, K) \in U$ and $b \geq -1$.

- $\lim_{s\to 0} I(s, \eta_0) > 0$ and $\lim_{s\to (y_M - y_m)} I(s, \eta_0) < 0$.

- Furthermore, for $(b, K) \in U$ and $b \geq 1$ we have

$$\frac{\mathrm{d}I(s, \eta_0)}{\mathrm{d}s} < 0. \tag{7.12}$$

Proposition 7.3

For system (2.2) *with* $0 < \varepsilon \ll 1$, *and* $(b, K) \in U$ *and* $b \geq -1$, *the following statements hold.*

(a) *The cyclicity of the slow-fast cycles with head in* Γ_S^m *is at most one. Furthermore, any canard cycle bifurcated from a slow-fast cycle belonging to* Γ_S^m *is stable.*

(b) *Inside* Γ_S^M, *there exists a unique slow-fast cycle, denoted by* $\gamma_s^M(s^*)$, *whose cyclicity is at most two. All the other slow-fast cycles belonging to* $\Gamma_S^M \setminus \{\gamma_s^M(s^*)\}$ *has cyclicity at most one. Furthermore, any canard cycle bifurcated from* $\gamma_s^M(s) \in \Gamma_S^M$ *with* $s \in (0, s^*)$(*resp.* $s \in (s^*, y_M - y_m)$) *is unstable (resp. stable).*

(a) For the cyclicity of the transitory slow-fast cycle, after careful calculations we realize that all the details are similar to the cyclicity of the slow-fast cycle without head.

(b) For the cyclicity of the common slow-fast cycle in T_{C}, by using the contraction map theorem we get that the common slow-fast cycle can bifurcate exactly one limit cycle, which is a relaxation oscillation.

Theorem 7.1

For system (2.2) *with* $0 < \varepsilon \ll 1$, *and* $(b, K) \in U$ *and* $b \geq -1$, *the following statements hold.*

(a) *The cyclicity of the slow-fast cycles without head in* $\Gamma^m_{\mathrm{U}} \cup \Gamma^M_{\mathrm{U}}$ *and of the transitory slow-fast cycles in* Γ^T_{U} *is at most one. Furthermore, the canard cycles bifurcated from the slow-fast cycles belonging to* $\Gamma^m_{\mathrm{U}} \cup \{(\mathrm{I}\text{-}3)\}$ (*resp.* $\Gamma^M_{\mathrm{U}} \cup \{(\mathrm{I}\text{-}8)\}$) *are stable* (*resp. unstable*).

(b) *The cyclicity of the slow-fast cycles with head in* Γ^m_{S} *is at most one, and the canard cycles bifurcated from the slow-fast cycles belonging to* Γ^m_{S} *are stable.*

Theorem 7.1

- (c) For the slow-fast cycles with head belonging to Γ_{S}^{M}, there exists a unique slow-fast cycle, denoted by $\gamma_{\mathrm{s}}^{M}(s^*)$, whose cyclicity is at most two, and the cyclicity of slow-fast cycles belonging to $\Gamma_{\mathrm{S}}^{M} \setminus \{\gamma_{\mathrm{s}}^{M}(s^*)\}$ is at most one. Furthermore, the canard cycles bifurcated from $\gamma_{\mathrm{s}}^{M}(s) \in \Gamma_{\mathrm{S}}^{M}$ with $s \in (0, s^*)$(resp. $s \in (s^*, y_M - y_m)$) is unstable (resp. stable).
- (d) The cyclicity of the common slow-fast cycle in Γ_{C} is one. Furthermore, the unique periodic orbit bifurcated from the common slow-fast cycle is hyperbolic and stable.
- (e) If one of the two contact points is a canard point and the other is a jump point, system (2.2) has at most two limit cycles which can be bifurcated from slow-fast cycles.

致谢

谢　　谢!

Thanks for your attention!